Finite Element Analysis of Generation and Detection of Lamb Waves Using Piezoelectric Transducers

Sorohan St., Constantin N., Anghel V. and Gavan M.

Politehnica University of Bucharest, Spl. Independentei 313, 060042, Bucharest, Romania
sorohan@form.resist.pub.ro

Abstract – The paper reports the use of Finite Element (FE) simulation and experiments meant to explore the operation conditions of the PieZoelectric wafer Transducer (PZT). Piezoelectrics is the coupling of structural and electric fields and may be solved using the multi-physics approach. Accordingly, three different multi-physics models were developed to investigate a plane strain problem. The first one includes two PZTs mounted on an aluminium plate and is used to model both the emission and reception signals. The next two ones are developed to separately model the emission and detection processes, in order to decrease the computational effort. The wave displacements are generated by a PZT-like actuator and the output voltage is obtained at a PZT receiver both by a multi-physics approach. The analysis considered the transducer lengths, the effects of the finite pulse width, the pulse dispersion and the detailed interaction between the piezoelectric element and the transmitting medium. The transmitted and received signals for so-called A0 and S0 modes have maxima close to the frequencies predicted in other works. A series of sensitivity curves relating the generation and receiving of Lamb waves were also determined and plotted as a function of the pulse center frequency and of the PZT lengths.
Keywords – Lamb wave, multi-physics finite element models, piezoelectric effect, piezoelectric transducers.

1 Introduction

Many authors considered the use of Lamb waves for non-destructive testing. Lamb waves can propagate on long distances in plates and tubes, making it possible to detect flaws over a considerable area by a set of transducers [5], [6]. Complications that are encountered include the existence of multiple modes and their dispersive character. A partial solution to this complexity is the use of transducers that excite only a single mode, and various strategies have been employed to this end [6]. Recently there has been increasing interest in the use of PZT wafers as transducers, mainly due to the simplicity and low cost of such transducers [2]. PZT wafers have been excited with continuous sinusoidal or pulse signals for defect detection in plates and the influence of flaws on the Lamb wave transmission has been modelled in trial simulations.
In most papers, the mechanical interactions between the PZT wafer and the structure

to be inspected are not directly included. Recently, it was observed that the wave emission and the reception using a PZT are physically distinct and both show a specific dependence on the pulse centre frequency [2], [3]. Taking the piezoelectric phenomena and the possible complicated geometry of the inspected items into account, a more accurate analysis of the whole coupled structural and electrical problem by the FE method is evaluated in this work.

2 Review of wave propagation and FE modelling

Piezoelectrics consists in the coupling of structural and electric fields, exploiting the natural material properties of quartz and of ceramics. A voltage difference applied to a piezoelectric material creates a displacement, and, reversely, vibrating a piezoelectric material generates a voltage difference. The electromechanical constitutive equations for linear material behaviour are [1], [7]:

$$\{T\} = [c]\{S\} - [e]\{E\}; \qquad \{D\} = [e]^T\{S\} + [\epsilon]\{E\}, \tag{1}$$

where $\{T\}$ is the stress vector, $\{D\}$ is the electric flux density vector, $\{S\}$ is the strain vector, $\{E\}$ is the electric field vector, $[c]$ is the elasticity matrix, $[e]$ is the piezoelectric stress matrix and $[\epsilon]$ is the dielectric matrix (evaluated at constant mechanical strain).

Using the variational principle, it is possible to derive a second order time-dependent system of equations that can be discretized using the FEM and that include the piezoelectric effect (for details see [1] and [7]):

$$\begin{bmatrix} [M] & [0] \\ [0] & [0] \end{bmatrix} \begin{Bmatrix} \{\ddot{u}\} \\ \{\ddot{V}\} \end{Bmatrix} + \begin{bmatrix} [C] & [0] \\ [0] & [0] \end{bmatrix} \begin{Bmatrix} \{\dot{u}\} \\ \{\dot{V}\} \end{Bmatrix} + \begin{bmatrix} [K] & [K_Z] \\ [K_Z{}^T] & [K_d] \end{bmatrix} \begin{Bmatrix} \{u\} \\ \{V\} \end{Bmatrix} = \begin{Bmatrix} \{F\} \\ \{L\} \end{Bmatrix} \tag{2}$$

where the submatrices and vectors used are: $[M]$-structural mass matrix; $[C]$-structural damping matrix; $[K]$-structural stiffness matrix; $[K_Z]$-piezoelectric stiffness matrix; $[K_d]$-dielectric coefficient matrix; $\{F\}$-applied nodal force vector; $\{L\}$-applied nodal charge vector; $\{u\}$-displacement vector; $\{V\}$-electric potential vector. The dot and double dots denote differentiation(s) with respect to time. To integrate this system, a full transient analysis using the Newmark method (with $\alpha = 0.25$, $\delta = 0.5$ and $\theta = 0.5$) was performed using ANSYS 7.0 code [7].

For a given PZT, the emitted and received wave modes depend on the applied signal frequency. This phenomenon is usually called mode selectivity and is particularly addressed. The obtained results provide more accurate predictions of the mode selectivity than previously reported ones using a simplified PZT model in the wave emission process [2]. Finally, this approach is readily adapted to explore the wave interactions with flaws and contour conditions.

In [3], for a similar study, a plate with thickness $h = 1.59$ mm has been used, together with a particular PZT. Here also several material properties have been made available. In our experiments we used the same input data for the numerical simulation, but allowed for different PZT dimensions. Simulations were made in the $100 - 600$ kHz range frequency. For the studied aluminium plate, only S0 and A0

Lamb modes (Fig. 1) exist at frequencies below 1 MHz, as it can be found on the dispersion curves in figure 2. Dispersion curves can be obtained by assuming a particular harmonic solution of the displacements into the Naviers equation for which the boundary conditions must be fulfilled. More detailed information about the dispersion curves can be found in [2], [4].

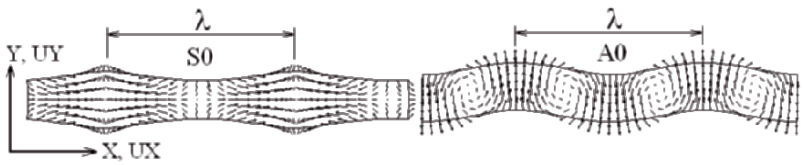

Fig. 1: Lamb modes in a plate. The wave propagates into X direction; λ denotes the wave length and the arrows show the instantaneous particle motion

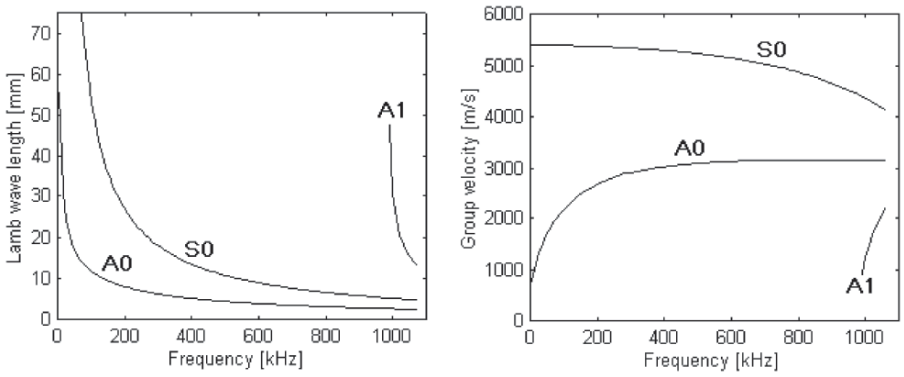

Fig. 2: Dispersion curves of an aluminium plate of 1.59 mm thickness

Figure 3 shows two similar wafer-type transducers bonded on an aluminium plate. The plate and the wafers are assumed to be of infinite extent in the Z direction (perpendicular to this paper), an ordinary plane strain assumption in structural mechanics. Only half of the plate was considered, with symmetry at the Y-axis. The wafer is a piezoelectric material with the poling direction normal to the surface of the plate and metallized on the top and bottom surfaces. The PZT actuation was excited with the pulse signal

$$V(t) = \begin{cases} 0.5V_0 \left[1 - \cos\left(\frac{2\pi f_0 t}{n_0}\right)\right] \cos(2\pi f_0 t); \text{ if } t \leq \frac{n_0}{f_0} \\ 0; \text{ if } t > \frac{n_0}{f_0} \end{cases} \tag{3}$$

where $V_0 = 10V$; the number of cycles $n_0 = 5$, and where the pulse centre frequency f_0 ranges between 100 and 600 kHz, is applied as input voltage between the metallized surfaces of the transducer (see Fig. 3).

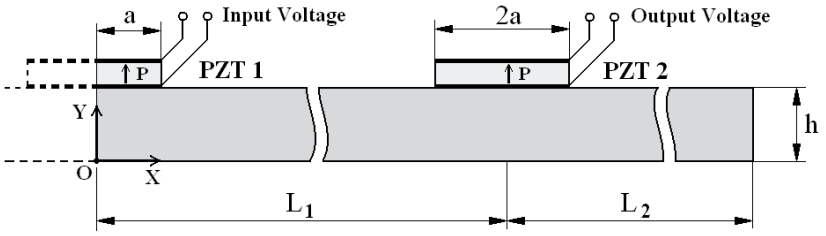

Fig. 3: The physical model used in finite element analysis

In FE simulations, the two PZTs and the plate were modelled individually using the PLANE13 element type within ANSYS. The Degrees Of Freedom (DOFs) of the two PZTs are the horizontal and the vertical displacements (UX and UY) and the electric potential (VOLT), while the DOFs of the plate are only UX and UY. The mesh parameters were chosen such that the element sizes were substantially smaller than a wavelength. Usually 10-20 elements per wavelength guarantee a good accuracy [7], in this case element size results between 0.2 and 0.4 mm (function of exciting frequency, see Fig.2a). The bottom surfaces of the PZTs were electrically grounded ($V = 0$) and an equipotential boundary condition was set on the top surfaces. Because the PZTs are bonded on the plate and the adhesive layer is neglected, the coincident nodes of the PZTs and the plate mesh were coupled both in X and Y direction. By symmetry, the X-displacement UX=0 at the origin. All other boundaries, except the input potential, were free. Simulations were performed in the time dependent mode with output time steps typically under one twentieth of a period $(0.1 - 0.25\mu s)$.

The above described approach more accurately matches with the actual PZT wafer /plate physical interaction. The generated 2D waves are propagating in the plate, inducing, by a similarly simulated interaction, an output voltage, collected at PZT 2. A simulation for a particular case ($L_1 = 200$ mm; $L_2 = 300$ mm; $2a = 6.4$ mm; average element size 0.4 mm - a total of 6333 nodes) shows the expected two propagating modes with S0 and A0 character (Fig. 4). The S0 mode has the highest group velocity (see also Fig.2) and shows particle displacements mostly in the X direction, and the slower A0 wave mode shows particle displacements mostly in the Y direction, asymmetric at the centre of the plate. It can be observed that the PZT 2 behaves like a reflecting flaw, converting the incident modes as physically must occur.

3 Emission of ultrasonic waves

In this section, simulations of the guided wave emission using PZT 1 as source are presented, putting in evidence the influence of the PZT length (2a in Fig. 3) upon the generated S0 and A0 Lamb modes. For reasons of computational effort, the model used in these simulations neglects the PZT 2 existing in figure 3, and considers a total plate length $L_1 + L_2 = 300$ mm. In order to quantify the variation of wave magnitudes with frequency, the maximum absolute value of UX for S0 mode and the maximum absolute value of UY for A0 mode were determined as maximum wave

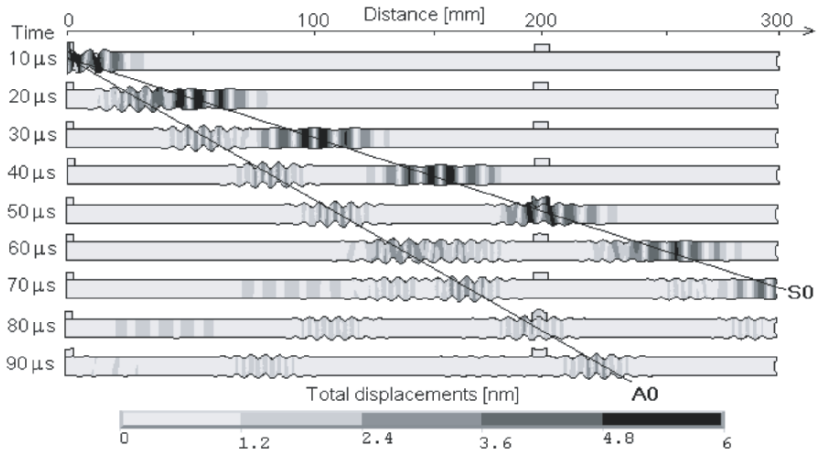

Fig. 4: Propagation of S0 and A0 modes at a central frequency of 300 kHz. The thickness of the plate has been exaggerated by a factor of 5 for improved visibility. The displacements have been scaled with a factor of 100000

magnitude when the two generated modes were clearly separated, for example at $t = 30\mu s$ in figure 4.

The sensitivity of generated waves, measured as maximum wave magnitude divided by the maximum input voltage, of about $V_0 = 10V$, is plotted in figure 5, separately for S0 and A0 mode, as a function of frequency bottom scale and Lamb wave length top scale, for different PZT lengths.

According to the simplified analytic model proposed by Giurgiutiu and Lyshevski [2], peak and null (or minimum) emission occur at wave length respectively, where *n* is an integer greater or equal to one. From relations (4) and dispersion curves (see Fig. 2a), the frequencies under 1 MHz, corresponding to maximum and minimum sensitivity, are determined and then summarized in the Tables 1 and 2, respectively.

$$\lambda^{(max)} = \frac{2a}{n - \frac{1}{2}}; \qquad \lambda^{(min)} = \frac{2a}{n}; \tag{4}$$

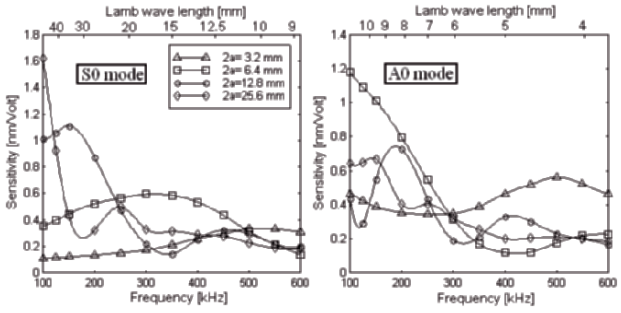

Fig. 5: The sensitivity to emission Lamb wave function of pulse centre frequency and PZT length

n	1		2		3		4	
2a[mm]	S0	A0	S0	A0	S0	A0	S0	A0
3.2	817.6	282.3	-	-	-	-	-	-
6.4	418.7	86.13	-	516.8	-	-	-	-
12.8	210.4	23.04	622.3	176.2	998.5	397.2	-	638.7
25.6	105.3	-	316.0	33.9	521.3	128.6	721.3	227.8

Table 1: Lamb wave fequencies [kHz] for maximum sensitivity as said by Eq. 4a

n	1		2		3		4	
2a[mm]	S0	A0	S0	A0	S0	A0	S0	A0
3.2	-	761.7	-	-	-	-	-	-
6.4	817.6	282.3	-	761.7	-	-	-	-
12.8	418.7	86.1	817.6	282.3	-	516.8	-	761.7
25.6	210.4	23.04	418.7	86.1	622.3	176.2	817.6	282.3

Table 2: Lamb wave fequencies [kHz] for minimum sensitivity as said by Eq. 4b

Comparing the results from figure 5 with the results from Table 1 and 2, a fair agreement between the Giurgiutiu & Lyshevski analytic results and the finite element results can be observed, especially for S0 mode.

4 Reception of Lamb waves

During the emission process, the complex motion of the plate and PZT 1 is symmetric about the Y axis and is later separated into S0 and A0 modes. During detection, the transducer interacts with a single mode which is propagating unidirectionally. Consequently, the displacements of PZT 2 will not be the same as during emission. Moreover, wave interaction with PZT generates additional reflected waves.
For computational effort reasons, the response of receiving PZT 2 was separately analysed for S0 and A0 modes. A particular S0 or A0 mode was selectively generated by adequately imposed displacements in interface nodes at X = 0. Therefore, PZT 1 was not included into the model and it was possible to consider $L_1 = 100$ mm and $L_2 = 100$ mm. The sensitivity of received waves (input voltage against maximum wave magnitude, measured by UX for S0 mode and UY for A0 mode) is plotted in figure 6.
It is clear that sensitivity increases as the PZT length decreases. However, especially for S0 mode, there are some optimal PZT lengths, function of the pulse centre frequency.

5 Global results and comparison with experiment

Figure 7 plots the ratio of the maximum received pulse amplitude to the exciting pulse amplitude as a function of frequency, namely the global sensitivity. Results are shown for four different transducer pairs, all separated by $L_1 = 200$ mm.
Measurements of the A0 and S0 wave amplitudes as a transfer functions have been

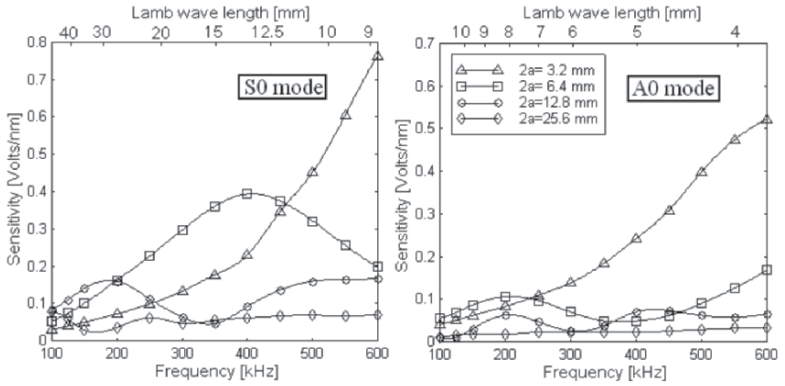

Fig. 6: The sensitivity to received Lamb wave function of pulse centre frequency and PZT length

reported in [3] only for $2a = 6.4$ mm and are in good agreement, in terms of frequencies for maximum sensitivity, with the results obtained during the numerical simulations presented in this work.

6 Conclusions

The operation of a PZT wafer transducer was analyzed for the generation and detection of guided Lamb waves using a multi-physics FE simulation and then compared with experiments reported in literature. The numerical simulations were intended to assess the possibility to follow a realistic mechanical interaction between the transducers and the transmitting inspected medium.

The results prove that multi-physics FE simulations are offering more accurate val-

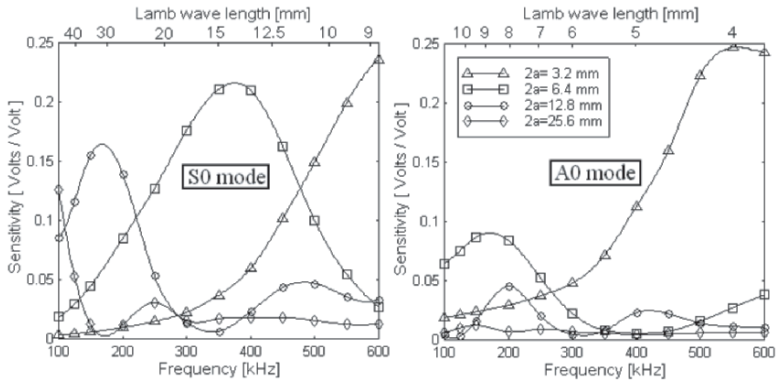

Fig. 7: The global sensitivity, or overall system transfer function $\frac{V_{out}}{V_{in}}$, as a function of pulse centre frequency and PZT length

ues for the peak frequencies and the mode selectivity. In addition, FE simulations

make it possible to determine the optimum transducer length, which may be different for emission and reception.

Acknowledgement

The research work was financed by Sure2Grip CRAFT project, run in FP6 programme under COOP-CT-2004-513266 contract.

References

[1] Allik, H., and Hughes, J. R.:Finite Element for Piezoelectric Vibration, International Journal for Numerical Methods in Engineering, **No. 2**, 151–157 (1970)

[2] Giurgiutiu, V., Lyshevski, S., E.: Micromechatronics: Modeling, Analysis, and Design with Matlab, **CRC Press**, (2004)

[3] Nieuwenhuis, J. H., Neumann, J., Greve, D. W., and Oppenheim, I. J.: Generation and detection of guided waves using PZT wafer transducers, IEEE Trans. Ultrasonics, Ferroelectrics, and Frequency Control, **Vol.52**, 2103–2111, (2005)

[4] Rose, J. L.:Back to basics - Dispersion curves in guided wave testing, Material Evaluation, **Vol.60**, 20–23,(2003)

[5] Rose, J. L.:Guided wave nuances for ultrasonic nondestructive evaluation, IEEE Trans. Ultrasonics, Ferroelectrics, and Frequency Control, **Vol.47**, 575–583, (2000)

[6] Zhongquing S., Lin, Y., Ye, L.:Guided Lamb waves for identification of damage in composite structures: A review, Journal of Sound and Vibration, **Vol.295**, 753–780, (2006)

[7] ***:Ansys, Inc. Theory. Reference and User Guides (2000)